Generation of Orbital Angular Momentum of Light and its application in Optofluidics

Gyanendra Yadav

A dissertation submitted for the partial fulfilment of BS-MS dual degree in Science

Indian Institute of Science Education and Research Mohali

April 2016

Certificate of Examination

This is to certify that the dissertation titled "Generation of Orbital Angular Momentum of Light and its application in Optofluidics" submitted by **Mr. Gyanendra Yadav** (Registration Number: **MS11058**) for the partial fulfillment of **BS-MS dual degree program** of the Institute, has been examined by the thesis committee duly appointed by the Institute. The committee finds the work done by the candidate satisfactory and recommends that the report be accepted.

Dr. Sanjeev Kumar	Prof. Sudeshna Sinha	Dr. Kamal P. Singh (supervisor)

April 22, 2016

Declaration

The work presented in this dissertation has been carried out by me under the guidance of Dr. Kamal P. Singh at the Indian Institute of Science Education and Research Mohali.

This work has not been submitted in part or in full for a degree, a diploma, or a fellowship to any other university or institute. Whenever contributions of others are involved, every effort is made to indicate this clearly, with due acknowledgement of collaborative research and discussions. This thesis is a bonafide record of original work done by me and all sources listed within have been detailed in the bibliography.

Mohali, April 22, 2016

Gyanendra Yadav

In my capacity as the supervisor of the candidate's project work, I certify that the above statements by the candidate are true to the best of my knowledge.

Mohali, April 22, 2016

Dr. Kamal P. Singh

Acknowledgement

I would like to express my gratitude to my supervisor, Dr. Kamal P. Singh for the useful comments, remarks and engagement through the learning process of this master thesis. I would also like to thank Gopal Verma for his endless assistance and motivation.

Furthermore, I would like to thank Dr. M.S. Siddhu and other lab members for their help during lab sessions. I would also like to thank my family for their unconditional love. I would like to thank my friends, Manu, Subbu, Hema, Sumit, Kishor, Akshay, Abhinav, Joydeep, Love and Bhati who in spare time helped me in making learning process joyful.

Last but not the least, I want to dedicate my thesis to those people of this country, who didn't have the privilege to study. I would consider my work successful if I happen to make significant contribution for them.

Contents

Abstract

Polarized light carries spin angular momentum but if we give azimuthal phase dependence to a light beam, it can carry well defined Orbital Angular Momentum(OAM). Laguerre Gaussian and Bessel beam are examples of this kind of light. In this thesis we generated Laguerre Gaussian modes of light which carries well defined Orbital Angular Momentum. We generated these modes through two methods-

- Through Spatial light Modulator(SLM). SLM is an electrically addressed, computer controlled device, which modulates the phase of light.

- Through spiral phase plate. It is made up of transparent material which has varying thickness around circumference but constant in radial direction.

After successfully generating different modes we detected and characterized OAM by taking diffraction pattern through single slit. This technique for sorting is not good enough for higher order LG modes.

Finally we explored the deformations on Graphene oxide surface caused by Gaussian laser beam and different modes of LG beam by using nanometric sensitive technique.

1

Introduction to Orbital Angular Momentum of light

Johannes Kepler deducted that comet's tail points away from the sun due to the linear momentum of light. In late 19th century Maxwell stated that light is an electromagnetic wave and carries momentum and energy. Later in 1909 Poynting suggested that circularly polarized Light carries spin angular momentum [Poy09]. The spin angular momentum is equal to $\pm\sigma\hbar$, where σ represents the two polarization state of light +1 and -1. In 1936 Beth was the first person to report that spin angular momentum can be transferred to birefringent wave plate [Bet36]. It was in 1992 when Allen *et al* pointed that light beams which have azimuthal phase dependence, can carry well defined orbital angular momentum which is independent to the polarization state [All+92]. The OAM is equal to $\pm l\hbar$, where l is the topological charge and can take values from $-\infty$ to $+\infty$. Topological charge(l) is equal to the number of twist light does in a wavelength [PA00].

The two common types of light beam which possess well defined OAM are Laguerre Gaussian beam and Bessel beam. We all know that in a normal Gaussian laser source light intensity is maximum at the center and decreases in radially outward direction. But in the case of LG and Bessel beam, due to helical phase fronts the intensity at the center becomes zero and the whole intensity lies on a ring shaped structure making it an optical vortex after taking projection on a surface. This is called phase singularity or screw dislocation.

1.1 Angular momentum of electromagnetic field

If the strength of electric field of light is E(r,t) and magnetic field density is B(r,t), the total linear momentum density [CCT97]

$$\vec{P} = \int (\epsilon_0 (\vec{E} \times \vec{B}) d^3\vec{r}) \tag{1.1}$$

taking cross product of this momentum with position vector $\vec{r}$, the total angular momentum

$$\vec{J} = \int (\epsilon_0 \vec{r} (\vec{E} \times \vec{B}) d^3\vec{r}) \tag{1.2}$$

taking $\vec{B} = \vec{\nabla} \times \vec{A}$ and using Coulomb Gauge($\vec{\nabla} \cdot \vec{A} = 0$) we get [Hra15]

$$\vec{J} = \int \epsilon_0 \Sigma|_{j=x,y,z} E_j (\vec{r} \times \vec{\nabla}) A_j d^3r + \int \epsilon (\vec{E} \times \vec{A}) d^3\vec{r}. \tag{1.3}$$

In coulomb gauge E and A have components only in the perpendicular plane to the propagation direction. Comparing eq. 3 with $\vec{J} = \vec{L} + \vec{S}$ we can say that 2nd term in eq. 3 is associated with SAM and it is independent from the choice of origin of coordinate system, therefore it is intrinsic in nature. The 1st term represents OAM. It can be both intrinsic and extrinsic in nature. It has been shown that if we choose origin on the beam axis in a coordinate system then the OAM associated to that will be intrinsic[O'N+02].

1.2 Laguerre Gaussian beams

Helmholtz equation is partial differential equation, which explains the time independent propagation of waves in free space. Therefore the complex amplitude $u(\vec{r})$ of any electromagnetic wave must satisfy this equation.

$$\nabla^2 u(\vec{r}) + k^2 u(\vec{r}) = 0 \tag{1.4}$$

where, k is the wavenumber of light and equal to $2\pi/\lambda$.

If we take paraxial approximation, the complex amplitude $u(\vec{r})$ will be equal to $u(\vec{r})\exp^{-ikz}$. Following the assumption that $u(\vec{r})$ slowly varies with z, we can write $\frac{\partial u}{\partial z}\lambda \ll u$ and $\frac{\partial^2 u}{\partial z^2}\lambda \ll^2 u$. Putting it in eq. (1.4)

$$(\frac{\partial^2 u}{\partial x^2} + \frac{\partial^2 u}{\partial y^2})u - 2ik\frac{\partial u}{\partial z} = 0 \tag{1.5}$$

If we solve the above equation in cylindrical coordinate system (ρ, ϕ, z) we get the complex amplitude for Laguerre Gaussian beam [EP04].

$$u_{p,l}(\rho,\phi,z) = A_{p,l}\frac{W(0)}{W(z)}(\frac{\rho}{W(z)})^{|l|}L_{p,l}^{|l|}(\frac{2\rho^2}{W^2(z)})exp(-\frac{\rho^2}{W^2(z)})$$
$$exp(-ikz - ik\frac{\rho^2}{R(z)} + i(|l|+2p+1\zeta(z))exp(-il\phi),$$

where $W(z) = W(0)\sqrt{1+(z/z_0^2)}$ is beam radius, $R(z) = z(1+(z/z_0^2))$ is wave-front curvature radius and $\zeta(z) = arctan(z/z_0)$ is Gouy phase with respect to a plane or spherical wave. $W(0) = \sqrt{\lambda z_0/\pi}$ and z_0 describes focusing of the beam. $L_{p,l}$ is associated generalized Laguerre polynomial.

This type of complex amplitude carrying beam is called Laguerre Gaussian beam of order (p,l). Here p, radial index, is a non negative whole number and called intrinsic hyperbolic momentum charge [PK15] and l, Azimuthal index, is the topological charge.

1.3 Comparison of intensity profile of Gaussian and LG beam

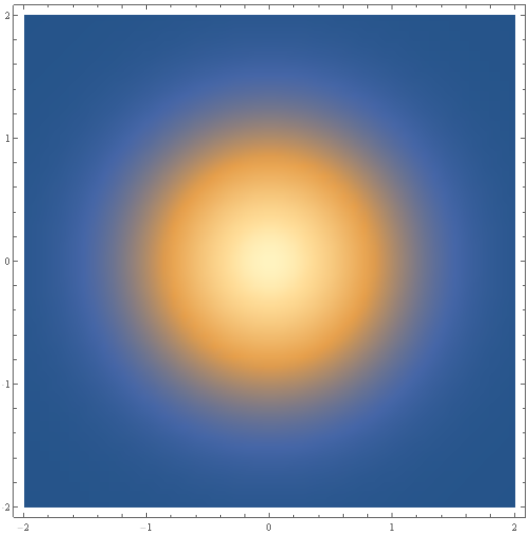

Fig. 1.1.: Numerical simulation of intensity profile of a gaussian beam(p=0, l=0) [@Zel14]. Here we can see that intensity at center is maximum and as we radially go outward, intensity decreases.

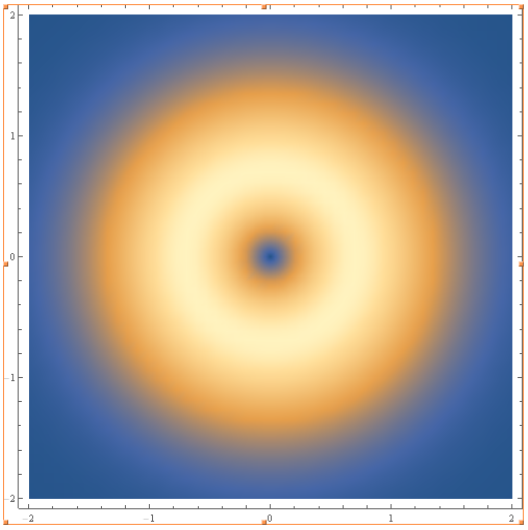

Fig. 1.2.: Numerical simulation of intensity profile of a LG beam(p=0, l=1). Here we can see phase singularity at center.

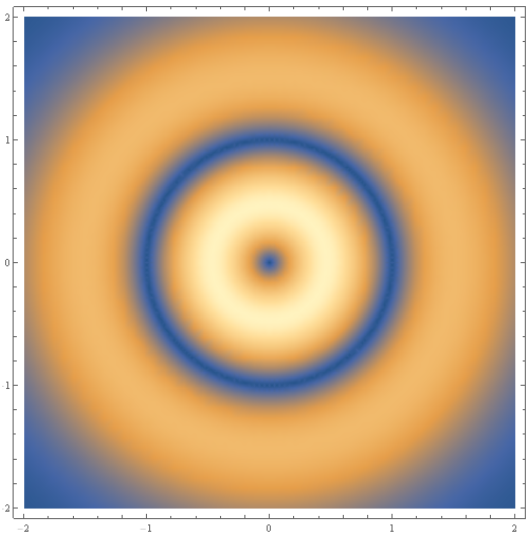

Fig. 1.3.: Numerical simulation of intensity profile of a LG beam(p=1, l=1). The number of rings will always be p+1.

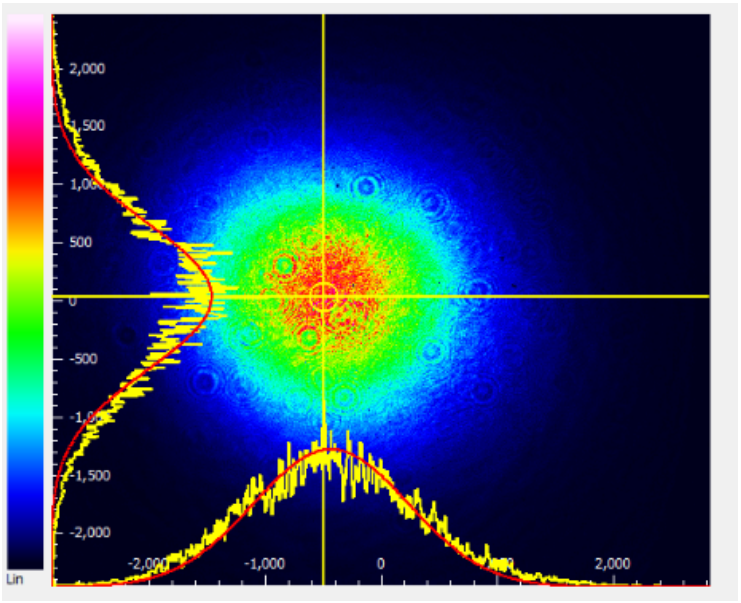

Fig. 1.4.: Beam profile image of Gaussian beam

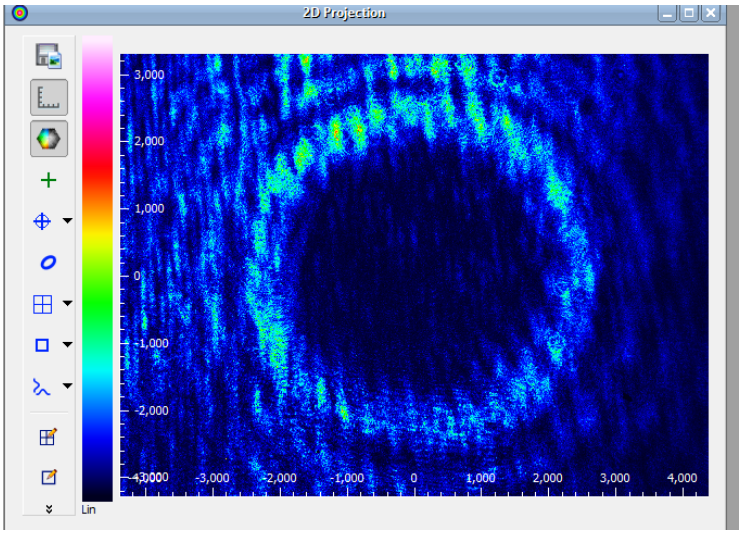

Fig. 1.5.: Beam profile image of Laguerre Gaussian beam

2

Generation and characterization of Laguerre Gaussian modes

Laguerre Gaussian beam can be generated by many ways. Few of those methods are by using cylindrical mode converters [CP99], spiral phase plate [Jai05], Spatial light modulator [Hra15], computer generated hologram, deformable mirror [Ren+10], birefringent liquid crystal plate(q plate) [Sue+04] etc. For our experiments we chose SLM and spiral phase plate to generate LG modes.

2.1 Generation through Spatial Light Modulator(SLM)

2.1.1 What is Spatial Light Modulator(SLM)?

A SLM is an electrically addressed transmissive or reflective(in our case reflective) device which is used to modulate phase and amplitude of light [Nef+90]. It is made up of liquid crystals. Liquid crystals are birefringent. It means liquid crystals have different refractive index in different directions. Inside the pixel of liquid crystals molecules align in helical twist formation,

where first and last molecules remains perpendicular to each other. After connecting the SLM to a computer, the signal from computer causes electric field across the pixels. Due to this, molecules aligns in the direction same as electric field. The property of birefringence and relative orientation of molecules forces the light to undergo different path length and henceforth to carry different phase. In short we can say that SLM creates controllable diffraction gratings. For the generation of LG modes we need to create fork shaped diffraction gratings.

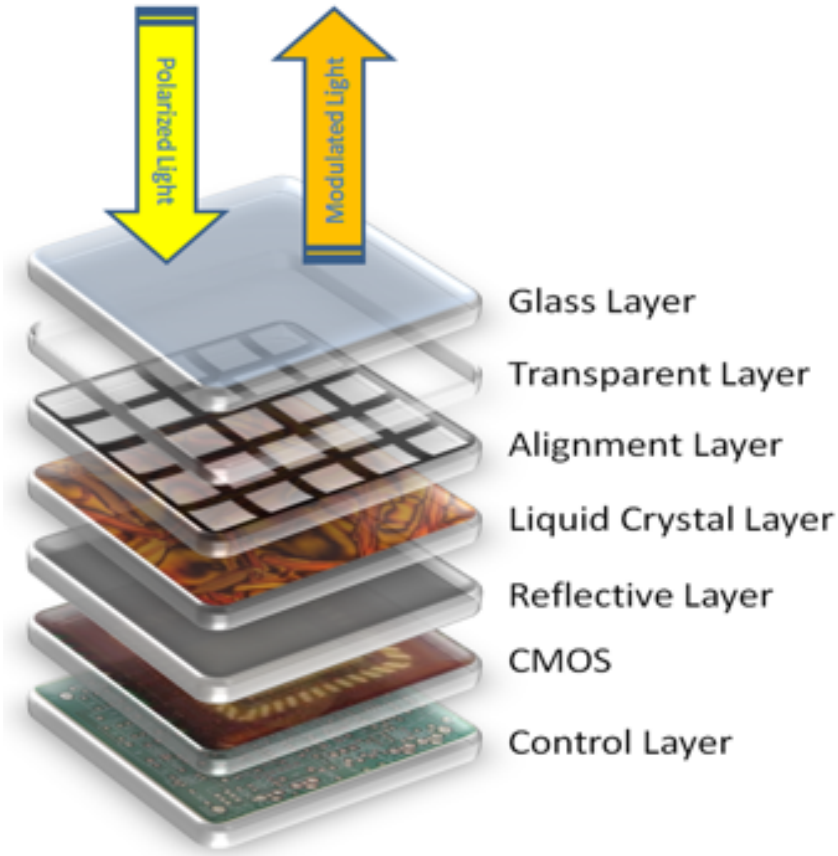

Fig. 2.1.: Different layers in SLM

2.1.2 Computer generated Hologram(CGH)

CGH is the phase pattern to convert a gaussian beam into desired LG beam. To make CGH we need to understand the concept of holography. Hologram is

a recorded interference pattern which has the information of both phase and intensity of object field. Unlike photography the image can be reconstructed from this recorded pattern even after removal of the object. To create a hologram we need to record the interference pattern on a photographic plate, of a reference beam and the beam coming from the object. After illuminating the recorded pattern with the reference beam, we get the desired copy of object in first diffracted order and it's complex conjugate in another first diffracted order. In zeroth order we get the reference beam.

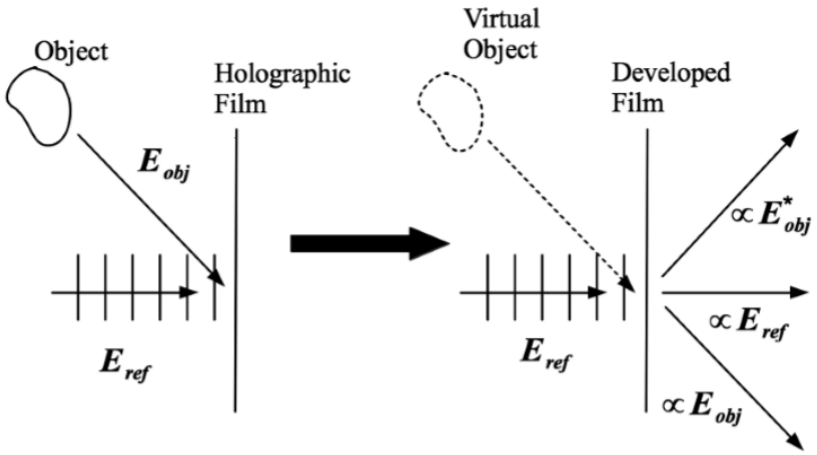

Fig. 2.2.: Working principle of a hologram [The]

The intensity pattern recorded on the hologram is

$$I = |E_{ref} + E_{obj}|^2 = E_{ref}^2 + E_{obj}^2 + 2Re[E_{ref} \cdot E_{obj}^*]. \tag{2.1}$$

In our case E_{ref} is for gaussian beam and E_{obj} is for LG beam.

The final phase distribution function to generate desired helical LG mode is given by this equation

$$I_p^l(r,\phi) = \pi\Theta(L_p^{|l|}(\frac{2r^2}{w_0^2})) + l\phi, \tag{2.2}$$

where Θ is Heaviside function and w_0 is the size of beam waist.

2.1.3 Blazed Phase grating profile

The light coming from SLM is comprised of both modulated and unmodulated components. The unmodulated light is the result of direct reflection from the upper layer of SLM. This unmodulated component propagates along the same axis as the modulated component which disturbs our output. Therefore to avoid this we need to add Blazed profile to our phase pattern. To add this mathematically we need to take modulo of 2π of the equation 2.2.

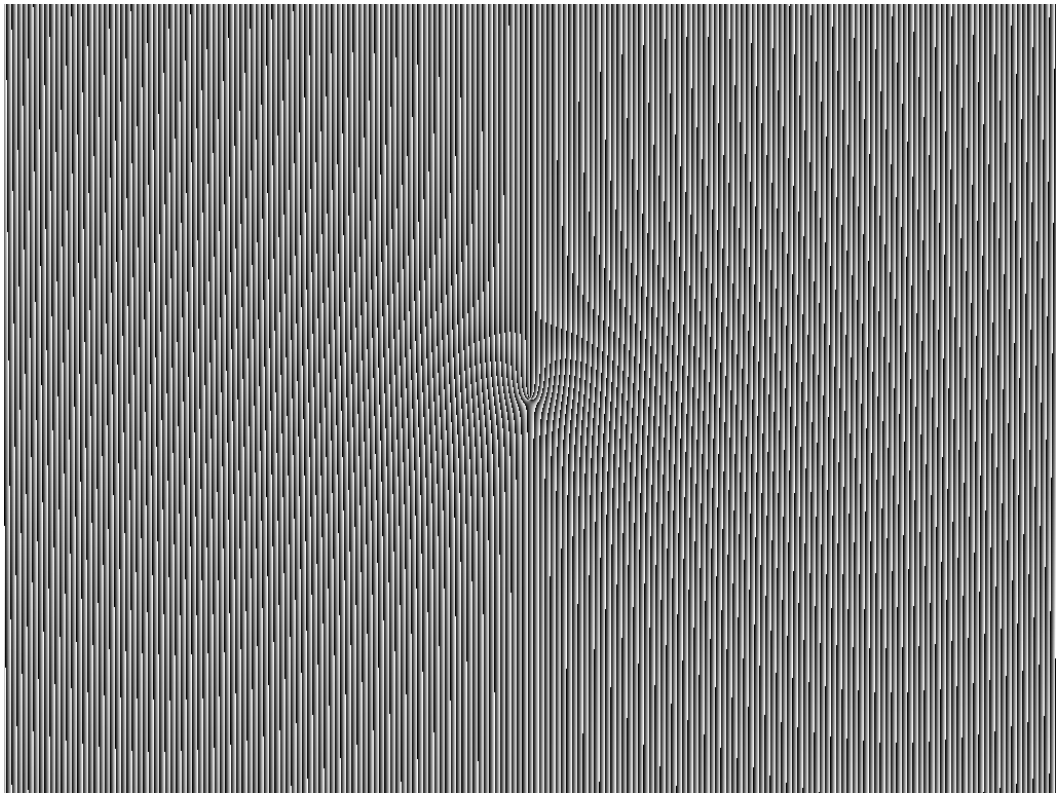

Fig. 2.3.: Phase profile to generate p=0, l=5 LG mode after blazing

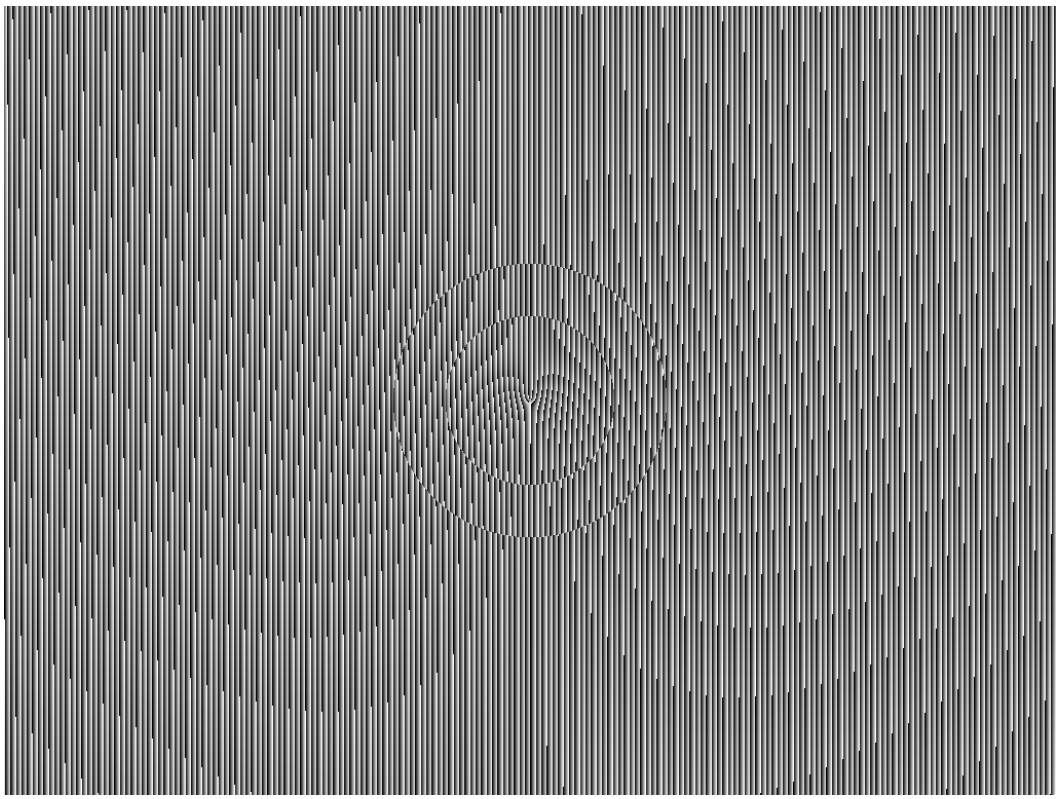

Fig. 2.4.: Phase profile to generate p=2, l=3 LG mode after blazing. Here number of circular discontinuity represents the radial index p.

2.1.4 Experimental setup to generate LG beam

To generate LG beam in laboratory we designed our setup according to Fig. 2.5 From one side we made incident gaussian beam of He-Ne laser on SLM which went through a half wave plate. We used half wave plate to achieve maximum diffraction efficiency. We imprinted our blazed phase profile on SLM by connecting it to computer. The spot size of incident beam and the width of hologram was adjusted such that we get maximum output power. After modulating through SLM, Gaussian light converted into LG beam. In the first diffracted order we got our desired LG mode. As we went further in diffraction order the value of topological charge(l) increased with nl, where n is the order of diffraction. We got the opposite charged LG beam in 2nd side of diffraction maxima. The central beam was Gaussian beam.

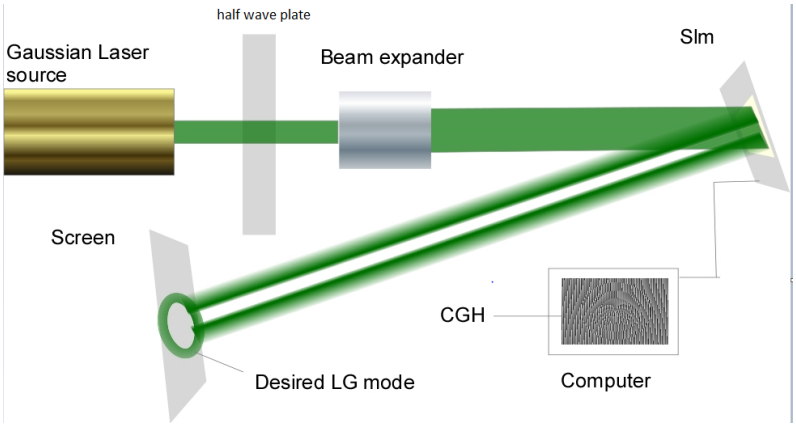

Fig. 2.5.: Ray diagram to generate LG modes

Fig. 2.6.: Tabletop setup to generate LG mode

2.1.5 Experimental Results

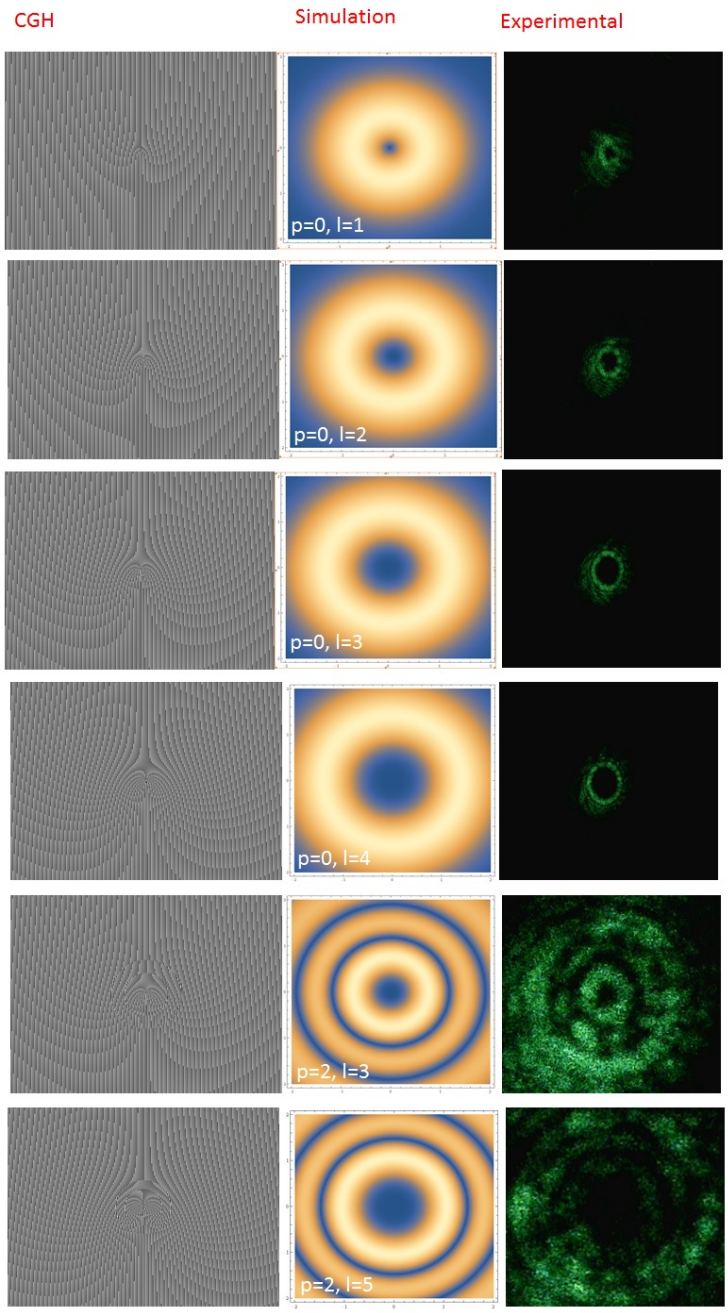

Fig. 2.7.: Generated different LG modes, their CGH and numerical simulation.

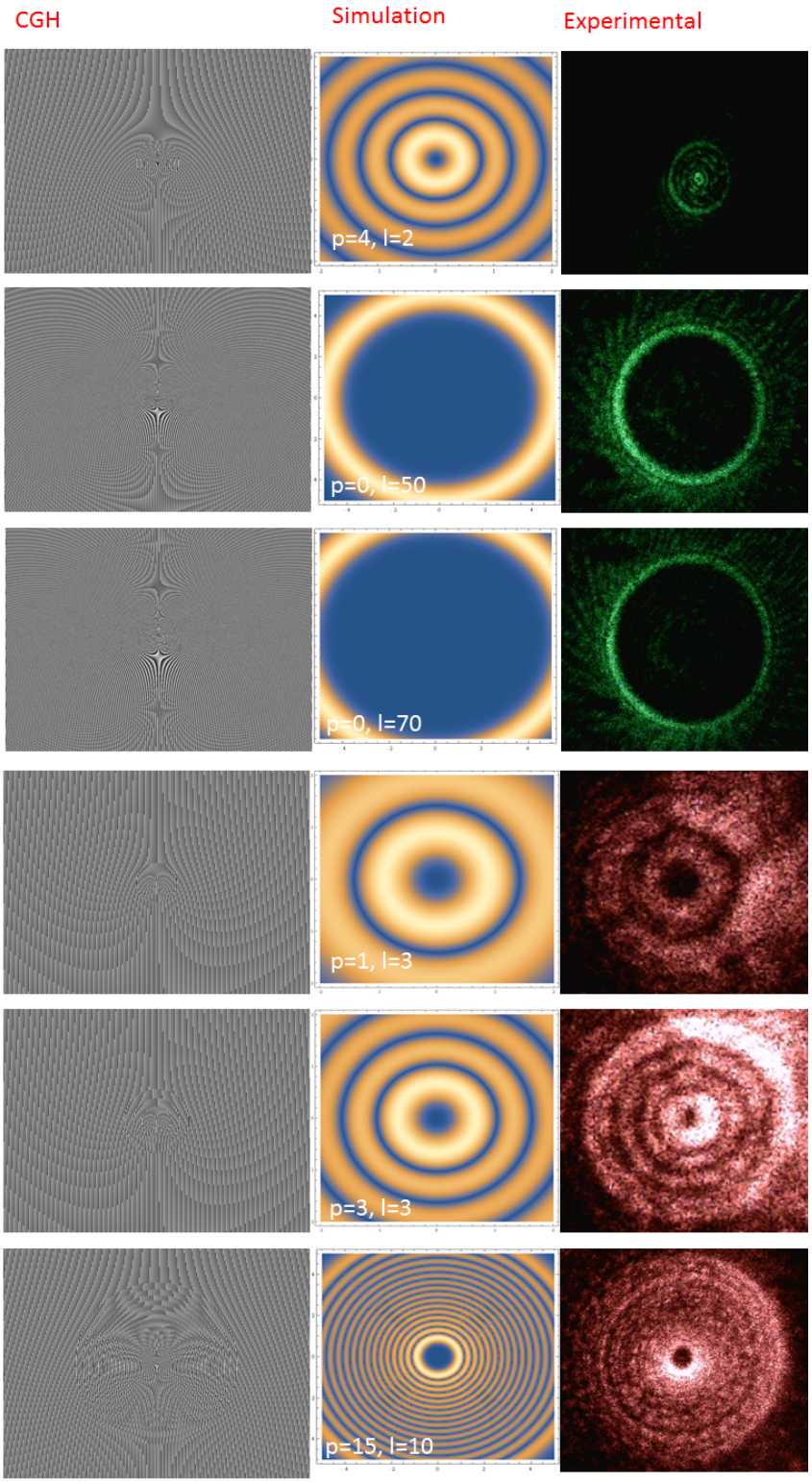

Fig. 2.8.: Generated different LG modes, their CGH and numerical simulation.

2.2 Generation through Spiral Phase Plate

To generate LG beam from gaussian beam we needed to impose azimuthal phase dependence to the structure of beam. This could be done directly through spiral phase plates. Spiral phase plate are made up of transparent material which has varying thickness in azimuthal direction. Due to this light travels different path at different points and associate a phase difference corresponding to each point. By adjusting the variation in thickness we can control the imposed phase factor.

Traditional spiral phase plates were costly. Therefore for our experiment to make an inexpensive phase plate we took microscope cover slip and cut it from one corner to the middle point and twisted the two planes which were formed due to cutting. It was an adjustable spiral phase plate because the phase dependence of light could be controlled by controlling the twisting angle. To generate LG beam from this, we just had to shine Gaussian laser light onto this.

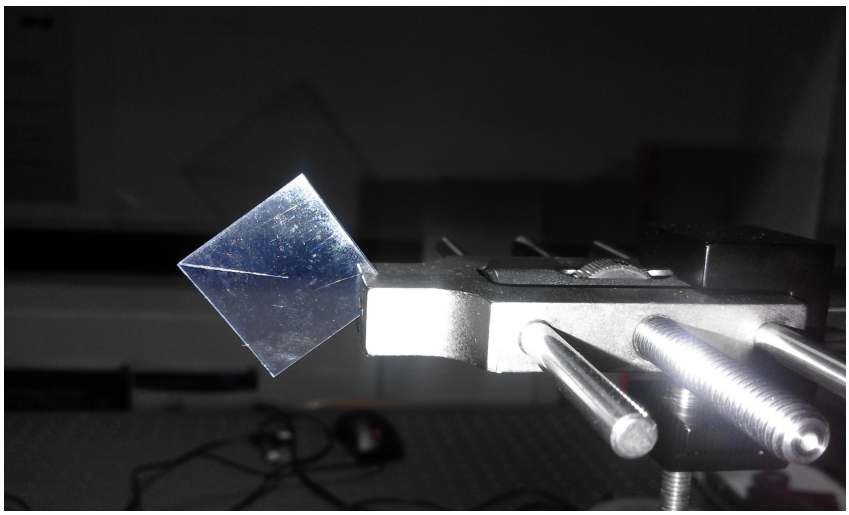

Fig. 2.9.: Microscope cover slip as an adjustable spiral phase plate to generate LG mode

Fig. 2.10.: Generated LG beam from microscope cover slip

2.3 Characterization of different OAM modes

OAM carrying beams had azimuthal dependence of phase, therefore their diffraction with single slit differed from that of Gaussian beam. Optical vortices are robust in nature when subjects to small perturbations. It doesn't destroy the vortex but shifts it's position. So when we passed the LG beam through single slit, by observing the shift in the fringes we could tell the topological charge of the beam [Gha+09].

2.3.1 Studying the diffraction pattern through single slit

Fig. 2.11 shows the diffraction pattern of Gaussian beam(l=0) after passing through single slit. Here we obtained straight line fringes.

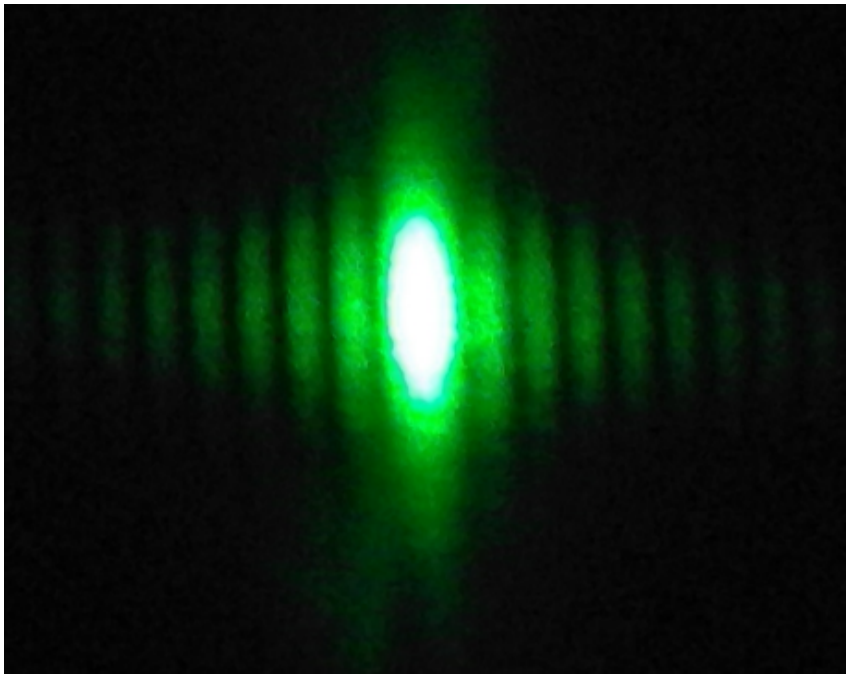

Fig. 2.11.: l=0

Fig 2.12 shows the diffraction pattern of l=2 LG beam after passing through single slit. Here we observed that first order bright(dark) fringe of the upper half part lied with the second order bright(dark) fringe of the lower half which was a characteristic of topological charge(l) +2 OAM mode.

Fig 2.13 shows the diffraction pattern of l=-2 LG beam after passing through single slit. Here we observed that after changing the sign of the topological charge from +2 to -2 the direction of shifting of fringes got reversed.

Fig. 2.14 shows the diffraction pattern of l=3 LG beam after passing through single slit. Here we observed that first order bright(dark) fringe of the upper

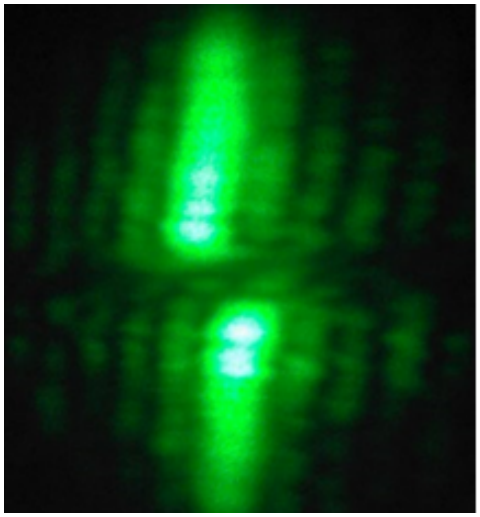

Fig. 2.12.: l=2

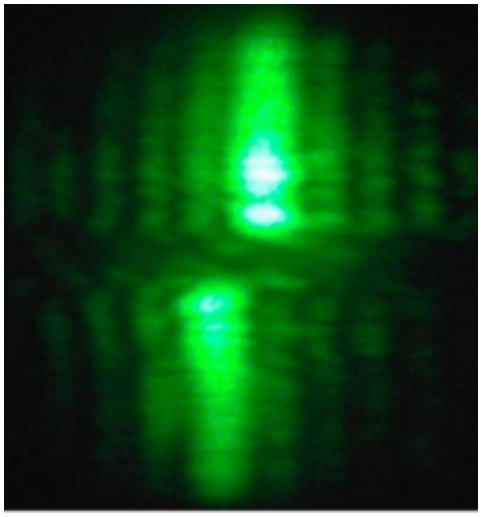

Fig. 2.13.: l=-2

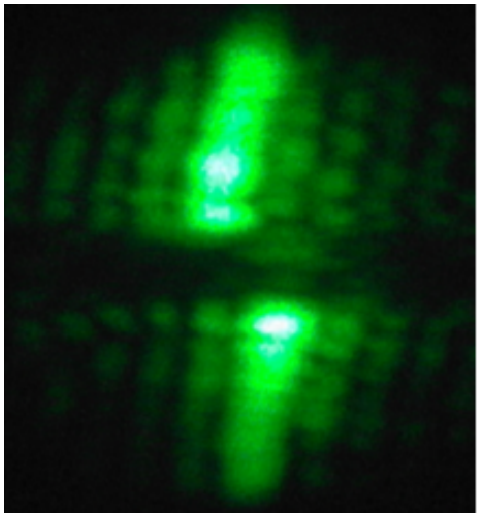

Fig. 2.14.: l=3

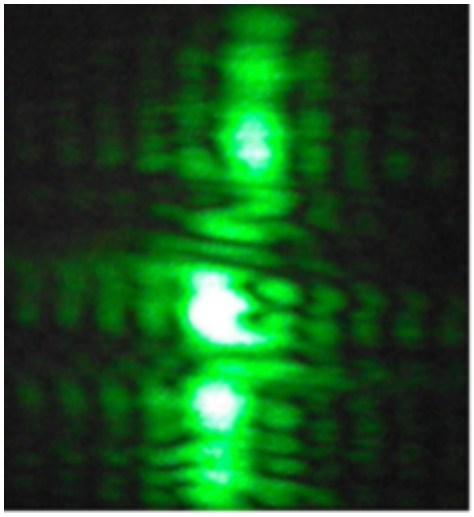

Fig. 2.15.: l=-2 from cover slip

half part lied with the third order dark(bright) fringe of the lower half which was a characteristic of topological charge(l) +3 OAM mode.

Fig. 2.15 shows the single slit diffraction pattern of LG beam generated through microscope cover slip. Here we observed that the topological charge was -2.

The technique which we used had it's own limitations. We couldn't characterize higher topological charged beam and couldn't became sure that there was no fractional OAM.

3

Application of light's OAM in optofluidics

After the generation and characterization of OAM in a light beam the first question raised about the applications of this structured light and its advantages over Gaussian beam. To check this on the Air fluid interface we designed an experiment where we compared the deformation on the surface caused by Gaussian beam and LG beam.

3.1 Design of the experiment

The list of apparatus and the devices used in our experiments are given in Appendix section. To calculate the deformations we used 2 laser light sources, one as a pump beam and other one as a probe beam. Pump beam was from dpss green(532nm) laser which had the power output range from 10mW to 6.5 watt. Probe beam was from He-Ne Red(632.8nm) laser which had the power output of around 15 mW. The liquid drop which we used was of graphene oxide. We arranged our experimental setup according to Fig. 3.1. We used nanometric sensitive technique [VS14] where we observed Newton ring type interference fringes of the light which were from the upper and lower surface of Graphene oxide drop. These fringes were dynamic due to the continuous evaporation of water present inside the drop of Graphene oxide. We received these fringes on a photodiode which was connected to an oscilloscope where we got the intensity versus time curve. After this we

gave shots of pump laser for both Gaussian and Laguerre Gaussian beam for different exposure time and observed the changes in intensity versus time plot on the oscilloscope. Both LG and Gaussian beams were tightly focused by a convex lens(focal distance = 25mm) before making incident on Graphene oxide drop. The spot size of the beams after tightly focusing was around $20\mu m$ to $25\mu m$. The setup presented in Fig. 3.1 and Fig. 3.2 is for LG beam, to give shots of Gaussian beam we replaced SLM to a mirror.

3.1.1 Experimental setup

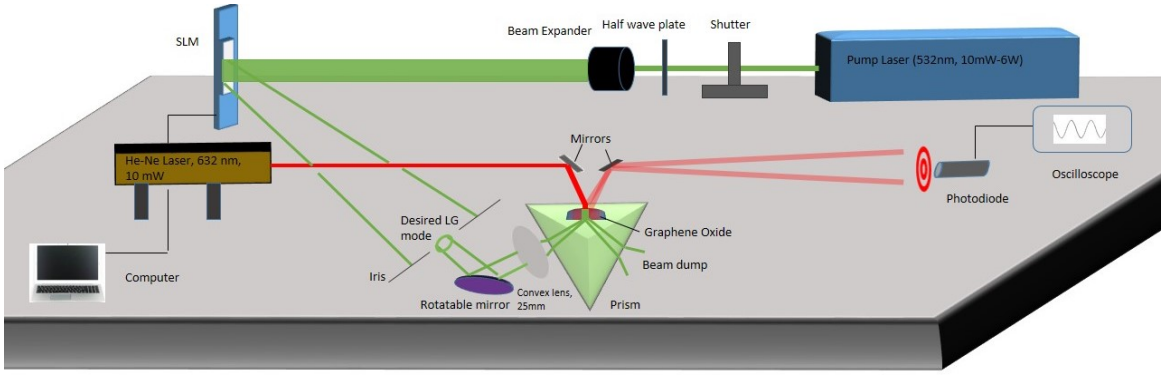

Fig. 3.1.: Arrangement of the setup on the optical bench

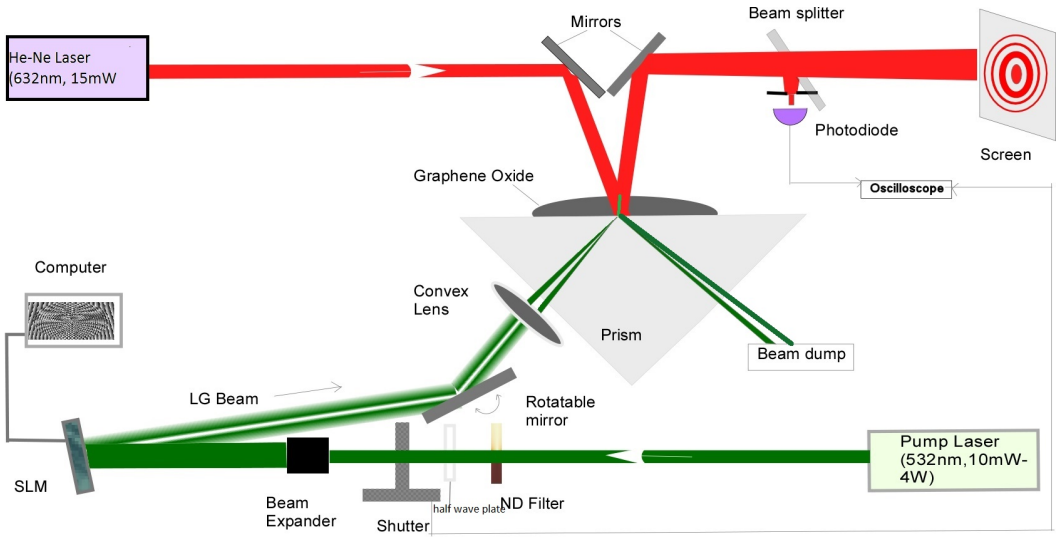

Fig. 3.2.: Ray diagram: Probe beam was made incident from the upper side of the prism surface. LG beam or Gaussian beam was made incident from below the graphene oxide drop.

3.1.2 Nanometric sensitive technique

To observe the deformation on the Graphene Oxide surface we used nanometric sensitive technique. In this technique we made newton ring shaped fringes like in Fig 3.3, by interfering the rays reflected from the lower and the upper surface of Graphene Oxide drop. The intensity, I(t) at the centre is proportional to $cos^2\left(\frac{4\pi n}{\lambda}d(t)\right)$, where n is the refractive index of the fluid, λ is the wavelength of incident light, d(t) is the height of the fluid from the surface of prism as a function of time. This is a noninvasive, self calibrating technique where the change in height of water surface during one minima to maxima is approximately $\lambda/4n \approx 118nm$. The amplitude of noise is less than 5 nm. Therefore we can easily measure deformations above 5nm.

3.1.3 Details of the graphene oxide solution

- Density: 0.981g/mL
- Refractive index: 1.333
- Concentration: 2mg/mL

3.2 Observations and Results

3.2.1 Difference in the direction and magnitude of deformation

LG beam produces more deformation than Gaussian beam and the direction of deforming the surface was opposite to that of gaussian beam.

Fig. 3.3 is the intensity versus time plot of evaporation fringes obtained from the drop of graphene oxide while giving shots of Gaussian beam. The intensity versus time plot is fitted by square of cosine curve. In this curve for the rising edge increased(decreased) intensity means that height of the drop is decreased(increased) and for the lowering edge increased(decreased) intensity means that height of the drop is increased(decreased). Here we observed that at the rising edge of wave, when shutter was open, intensity decreased with time. It means in this case height of the drop is increased(bump).

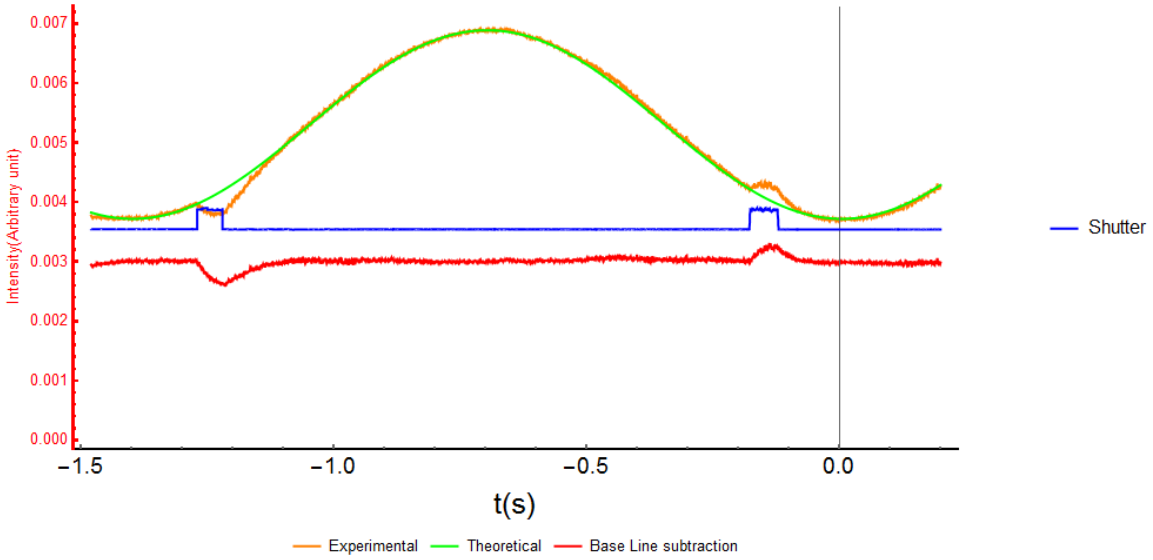

Fig. 3.3.: Incident beam:Gaussian, l=0, Power=150mW, Spot size≈ $25\mu m$, Drop volume≈ $50\mu L$, Drop diameter = 3to5mm, Shutter opening duration=100ms, Deformation height≈11nm.

Fig. 3.4 is the same plot for the case of LG beam. We observed that height of the drop decreased(dip) when the shutter was open.

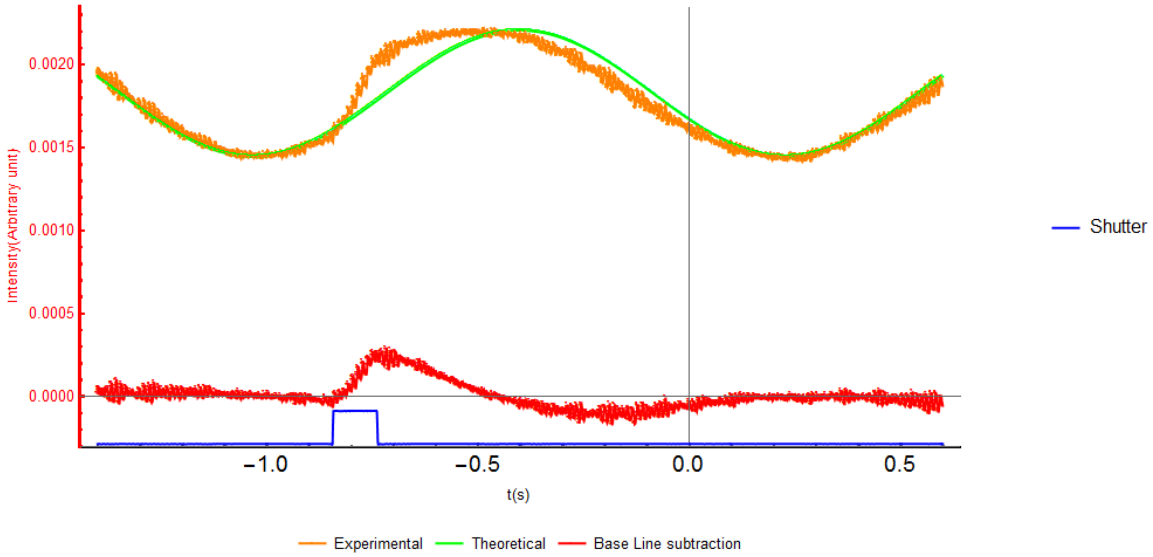

Fig. 3.4.: Incident beam:LG, l=1, Power=55mW, Spot size≈ $25\mu m$, Drop volume≈ $50\mu L$, Drop diameter = 3to5mm, Shutter opening duration=100ms, Deformation height≈30nm.

3.2.2 Heating effect

To confirm that there is transfer of heat from Graphene to water we varied the shutter duration and decreased the laser power.

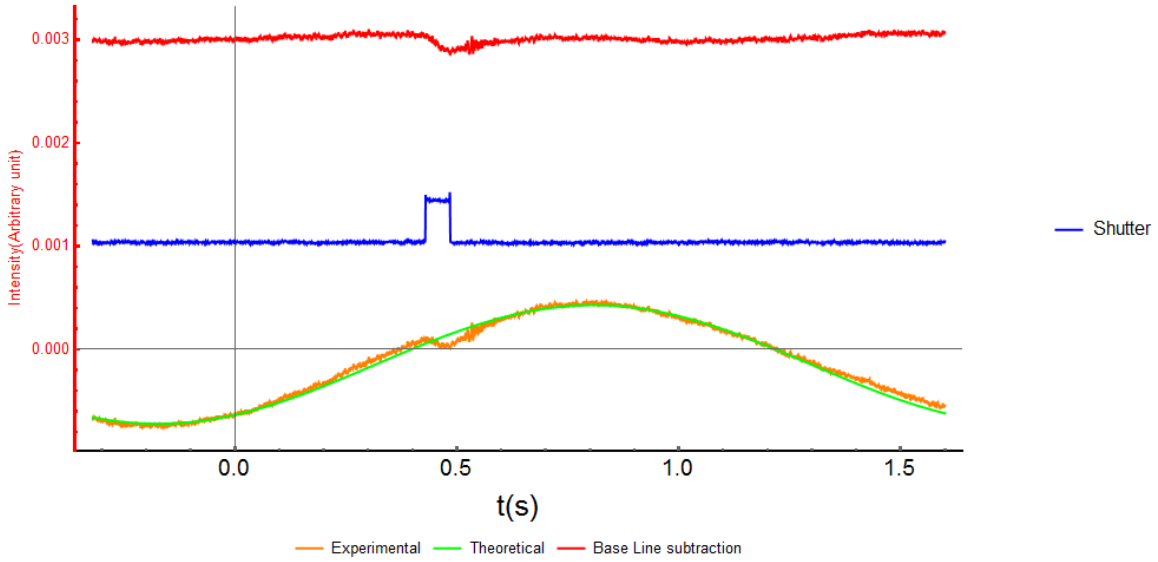

Fig. 3.5.: Incident beam:Gaussian, l=0, Power=100mW, Spot size$\approx 25\mu m$, Drop volume$\approx 50\mu L$, Drop diameter = 3to5mm, Shutter opening duration=50ms

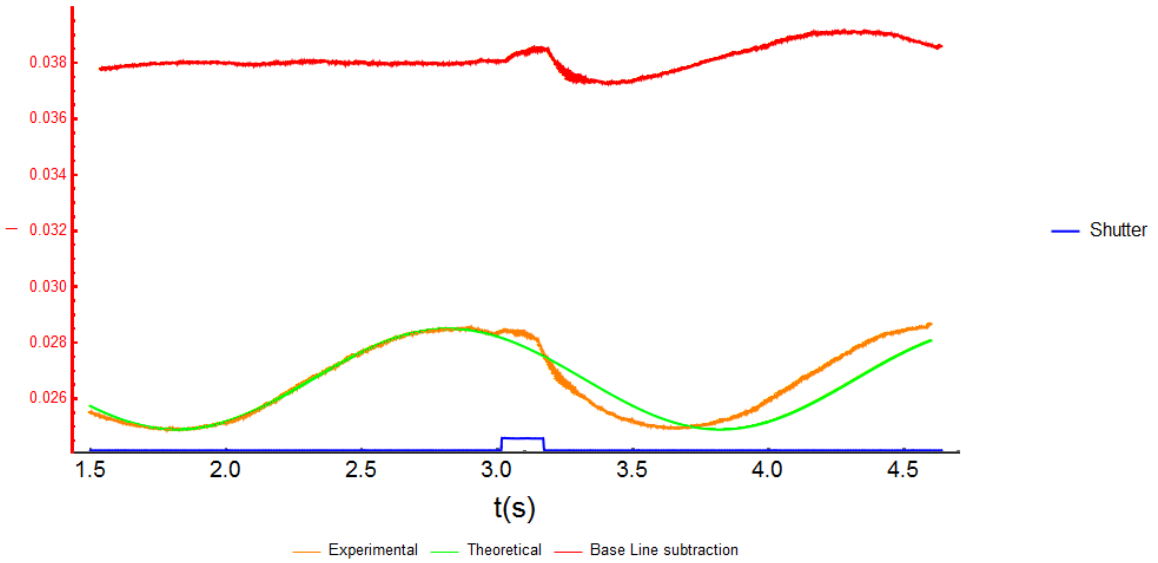

Fig. 3.6.: Incident beam:Gaussian, l=0, Power=100mW, Spot size$\approx 25\mu m$, Drop volume$\approx 50\mu L$, Drop diameter = 3to5mm, Shutter opening duration=150ms

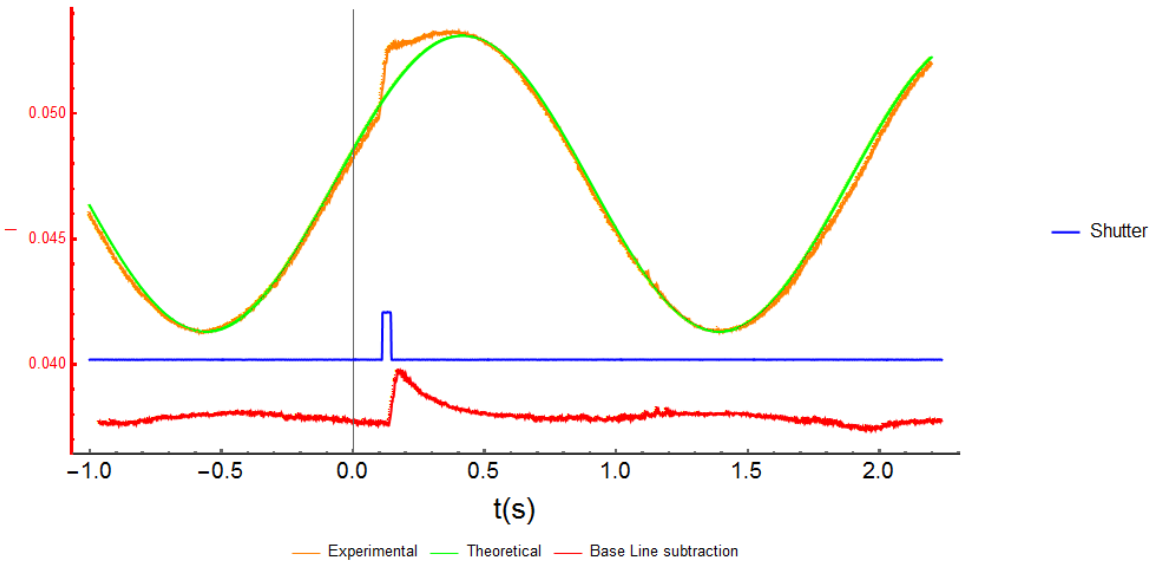

Fig. 3.7.: Incident beam:LG, l=1, Power=25mW, Spot size≈ $25\mu m$, Drop volume≈ $50\mu L$, Drop diameter = 3to5mm, Shutter opening duration=30ms

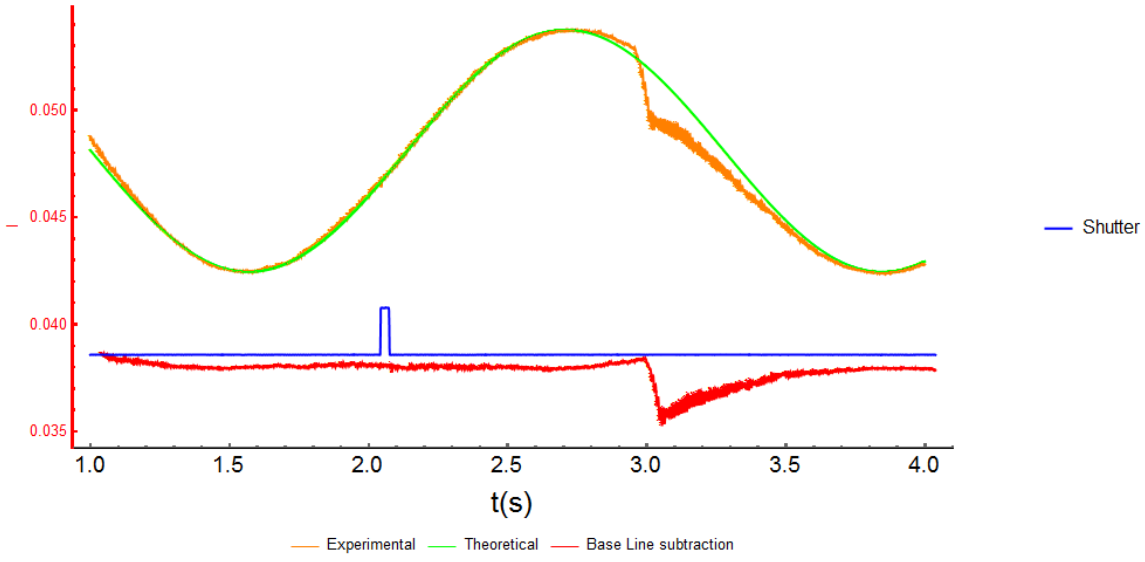

Fig. 3.8.: Incident beam:LG, l=1, Power=25mW, Spot size≈ $25\mu m$, Drop volume≈ $50\mu L$, Drop diameter = 3to5mm, Shutter opening duration=50ms

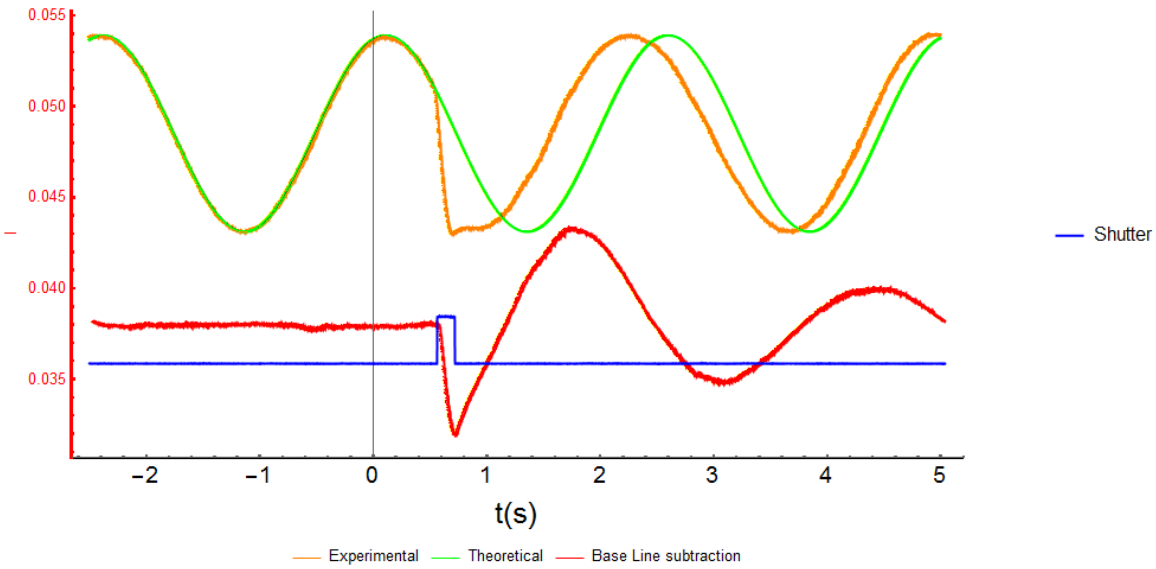

Fig. 3.9.: Incident beam:LG, l=1, Power=25mW, Spot size≈ $25\mu m$, Drop volume≈ $50\mu L$, Drop diameter = 3to5mm, Shutter opening duration=150ms

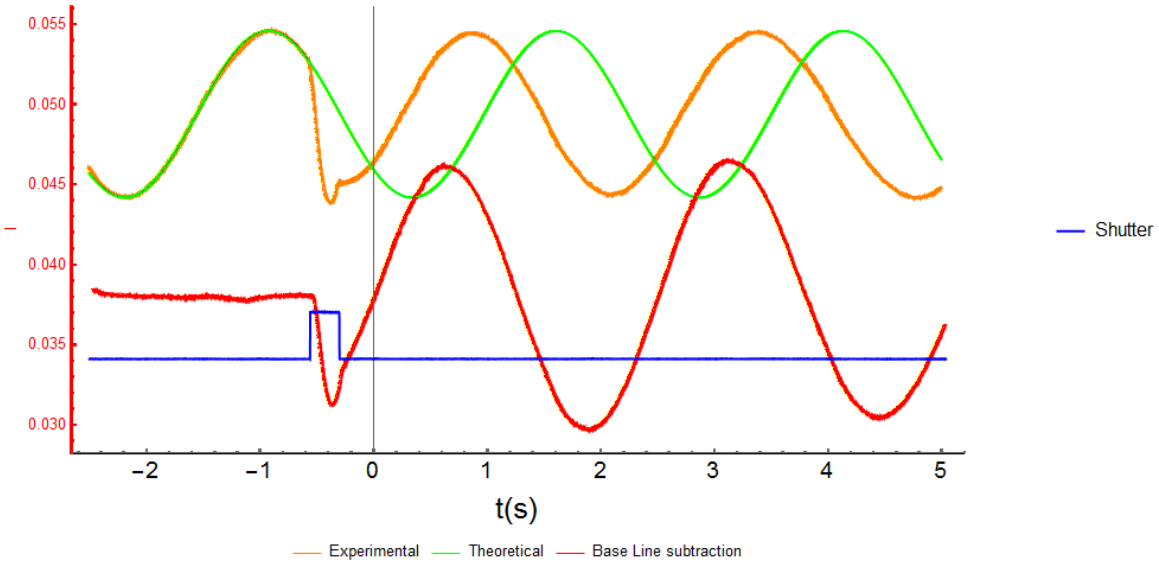

Fig. 3.10.: Incident beam:LG, l=1, Power=25mW, Spot size≈ $25\mu m$, Drop volume≈ $50\mu L$, Drop diameter = 3to5mm, Shutter opening duration=250ms

In Fig. 3.5 and Fig. 3.6, we gave the shot of gaussian beam(l=0) of 50ms and 150ms respectively. We observed that the slope of graph during the opening time of shutter is not the same as it was before opening the shutter. It means that heating effect was dominating the effect of radiation pressure. At 150ms shutter duration heating effect increased.

In Fig. 3.7, 3.8, 3.9, 3.10, we gave laser shots of LG beam(l=1) for the shutter duration of 30ms, 50ms, 150ms, 250ms respectively. For 150ms and 250ms the slope of the curve after opening the shutter couldn't come to the slope before opening the shutter even after one and two cycles respectively.

From these figures we deduced that graphene had very fast optical response in tranferring heat to the water because even for 30ms and 50ms the evaporation rate was changed.

3.2.3 OAM value versus deformation amplitude

We varied OAM values for the same configuration as Fig. 3.4. We observed that as we increased OAM value, the deformation amplitude decreased and the deformation amplitude was almost same for +l and -l.

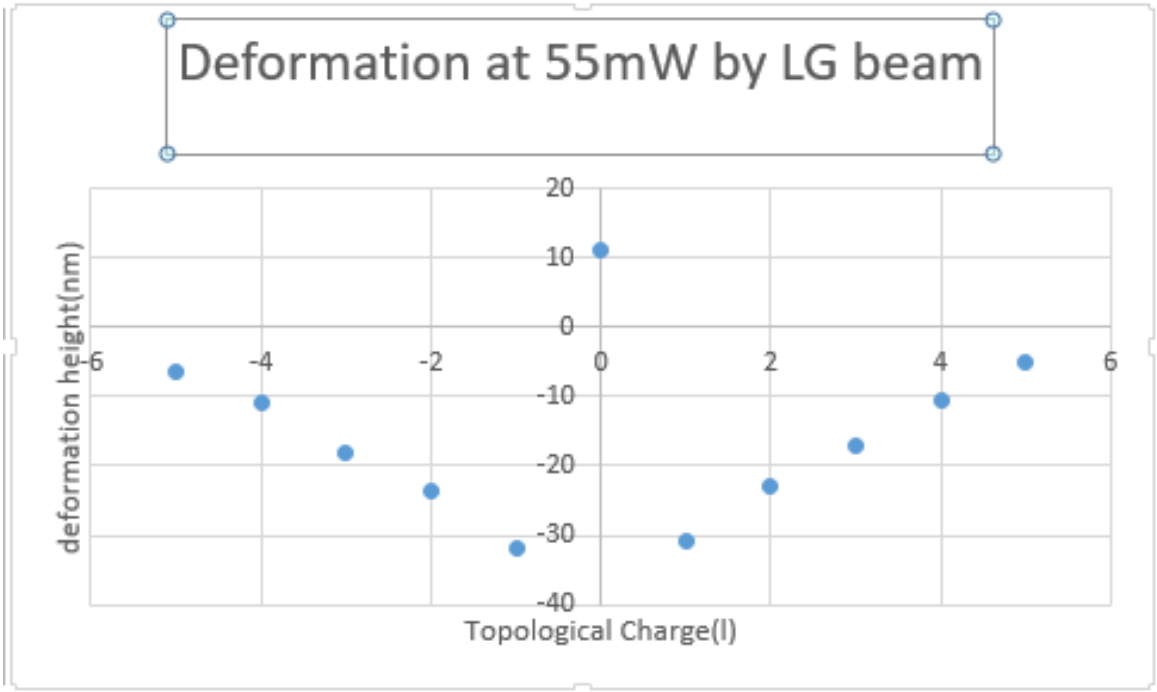

Fig. 3.11.: Deformation amplitude versus topological charge

3.3 Cross checks

• There was a possibility that the difference in amplitude and direction of deformation might be due to the hollow intensity profile of the beam, not the transfer of angular momentum. To counter check this possibility we produced same intensity pattern from Gaussian beam by using reflective objective.

We observed that the deformation direction and amplitude caused by the beam which had this type of intensity pattern, was similar to that of Gaussian beam. This result confirms that the opposite and greater deformation

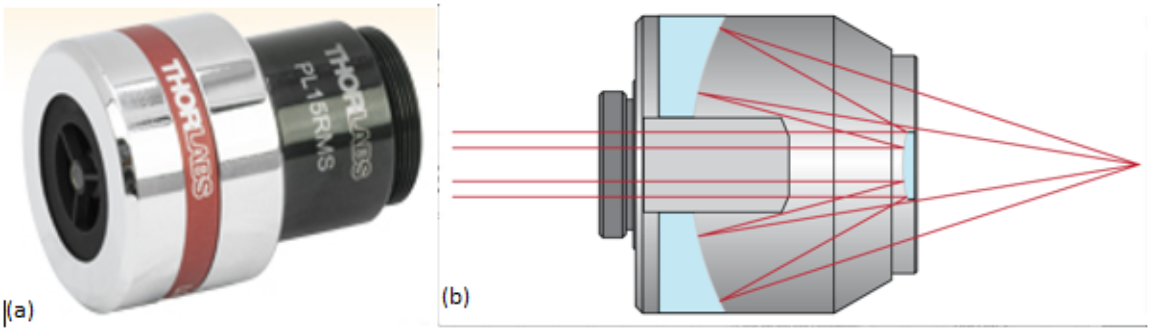

Fig. 3.12.: (a)Reflective objective, (b)Beam diagram [@Lab13]

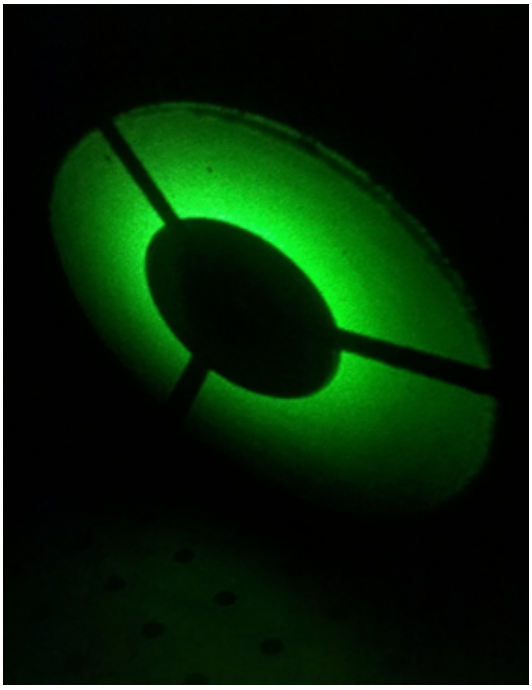

Fig. 3.13.: Intensity pattern of beam produced by all reflective objective

amplitude in case of LG beam is due to the transfer of angular momentum, not the intensity profile.

• The second possibility was that the invert and large deformation produced by LG beam could also occur due to the transfer of SAM. To check this we used a quarter wave plate and made circularly polarized Gaussian beam which carried spin angular momentum of $+\hbar$ or $-\hbar$. Again in this case the deformation was similar to that of linearly polarized Gaussian beam.

From these two cross checks we deduced that invert and large deformation produced by LG beam compared to that of Gaussian beam was due to the transfer of OAM.

4

Conclusion

In this thesis we have used two simple techniques to generate OAM in a Gaussian beam of light. We have shown that we can generate any OAM mode of Laguerre Gaussian beam of light and were able to sort out few OAM modes. While experimenting with liquid drops we were able to clearly observe the differences in deformation amplitude in nanaometric scale produced by Gaussian beam and LG beam. By using the nanometric sensitive technique we were able to conclude that with increasing the value of OAM, the deformation amplitude decreases. We have shown that only by adding the phase dependence in a light beam the absorptivity, in Graphene Oxide drop can be increased.

It's not more than 25 years has passed, since the understanding that light beams possessing OAM can be generated in the laboratory, therefore this field has tremendous mysteries to be explored.

4.1 Open questions

• What is the mechanism of heat transfer from laser light to water through Graphene?
• What is the selection rule for transitions taking place in case of operating with OAM carrying beam?.

Appendices

A

Devices and materials used in experiments

- DPSS green(532nm) laser with variable power output
- He-Ne red(632.8nm) gas laser
- Shutter and shutter controller
- Oscilloscope
- Photodiodes with wavelength filter
- Spatial Light Modulator(for visible range)
- Computer
- Half wave plate, Quarter wave plate
- Beam expander
- Mirrors and mounts
- Prism and prism holder
- HDMI and VGA cable
- Convex lens(focal distance 25mm)
- Aperture and iris
- Neutral-density filter
- Micro pipette
- Power meter
- Beam profiler
- Lens cleaning tissue
- All reflective mirror
- Vibrationless optical table
- Graphene Oxide

A.1 Details of Spatial Light Modulator

The SLM which we used was HOLOEYE PLUTO phase only spatial light modulator. It was a reflective LCOS, which had a resolution of 1920×1080, pixel size = 8.0 μm, 93% fill factor, Active area=$15.36 \times 8.64mm$. The addressing was 8 bit(256 Grey levels).

Bibliography

[All+92] L. Allen, M. W. Beijersbergen, R. J. C. Spreeuw, and J. P. Woerdman. „Orbital angular momentum of light and the transformation of Laguerre-Gaussian laser modes“. In: *Phys. Rev. A* 45 (11 1992), pp. 8185–8189 (cit. on p. 1).

[Bet36] Richard A. Beth. „Mechanical Detection and Measurement of the Angular Momentum of Light“. In: *Phys. Rev.* 50 (2 1936), pp. 115–125 (cit. on p. 1).

[CCT97] G. Grynberg C. Cohen-Tannoudji J. Dupont-Roc. *Photons and Atoms: Introduction to Quantum Electrodynamics*. Wiley, 1997 (cit. on p. 2).

[CP99] J. Courtial and M.J. Padgett. „Performance of a cylindrical lens mode converter for producing Laguerreâ€“Gaussian laser modes“. In: *Optics Communications* 159.1â€“3 (1999), pp. 13 –18 (cit. on p. 7).

[EP04] Jörg Enderlein and Francesco Pampaloni. „Unified operator approach for deriving Hermite–Gaussian and Laguerre–Gaussian laser modes“. In: *J. Opt. Soc. Am. A* 21.8 (2004), pp. 1553–1558 (cit. on p. 3).

[Gha+09] Devinder Pal Ghai, P. Senthilkumaran, and R.S. Sirohi. „Single-slit diffraction of an optical beam with phase singularity“. In: *Optics and Lasers in Engineering* 47.1 (2009), pp. 123 –126 (cit. on p. 16).

[Hra15] Mateja Hrast. *Orbital angular momentum of light*. 2015 (cit. on pp. 2, 7).

[Jai05] Amol Jain. *Creation of Optical Vortices Using an Adjustable Spiral Phase Plate and Computer-Generated Holograms*. 2005 (cit. on p. 7).

[Nef+90] J. A. Neff, R. A. Athale, and S. H. Lee. „Two-dimensional spatial light modulators: a tutorial“. In: *Proceedings of the IEEE* 78.5 (1990), pp. 826–855 (cit. on p. 7).

[O'N+02] A. T. O'Neil, I. MacVicar, L. Allen, and M. J. Padgett. „Intrinsic and Extrinsic Nature of the Orbital Angular Momentum of a Light Beam“. In: *Phys. Rev. Lett.* 88 (5 2002), p. 053601 (cit. on p. 2).

[PA00] Miles Padgett and L. Allen. „Light with a twist in its tail“. In: *Contemporary Physics* 41.5 (2000), pp. 275–285. eprint: http://dx.doi.org/10.1080/001075100750012777 (cit. on p. 1).

[PK15] William N. Plick and Mario Krenn. „Physical meaning of the radial index of Laguerre-Gauss beams“. In: *Phys. Rev. A* 92 (6 2015), p. 063841 (cit. on p. 3).

[Poy09] J. H. Poynting. „The Wave Motion of a Revolving Shaft, and a Suggestion as to the Angular Momentum in a Beam of Circularly Polarised Light“. In: *Proceedings of the Royal Society of London A: Mathematical, Physical and Engineering Sciences* 82.557 (1909), pp. 560–567. eprint: http://rspa.royalsocietypublishing.org/content/82/557/560.full.pdf (cit. on p. 1).

[Ren+10] Yu-Xuan Ren, Ming Li, Kun Huang, et al. „Experimental generation of Laguerre-Gaussian beam using digital micromirror device“. In: *Appl. Opt.* 49.10 (2010), pp. 1838–1844 (cit. on p. 7).

[Sue+04] K. Sueda, G. Miyaji, N. Miyanaga, and M. Nakatsuka. „Laguerre-Gaussian beam generated with a multilevel spiral phase plate for high intensity laser pulses“. In: *Opt. Express* 12.15 (2004), pp. 3548–3553 (cit. on p. 7).

[The] (Cit. on p. 9).

[VS14] Gopal Verma and Kamal P. Singh. „Time-resolved interference unveils nanoscale surface dynamics in evaporating sessile droplet“. In: *Applied Physics Letters* 104.24, 244106 (2014) (cit. on p. 19).

Websites

[@Lab13] Thor Labs. *Reflective Microscope Objectives*. 2013. URL: http://www.thorlabs.com/images/TabImages/Reflective_Objective_Beam_Diagram_800.gifl (cit. on p. 29).

[@Zel14] Enrique Zeleny. *Laguerre-Gaussian Modes of Paraxial Wave Equation*. 2014. URL: http://demonstrations.wolfram.com/LaguerreGaussianModesOfParaxialWavel (cit. on p. 4).

[@Fre10] Free Software Foundation, Inc. *GNU General Public License*. 2010. URL: http://www.gnu.org/licenses/gpl.html (visited on May 27, 2011).

List of Figures